Nuclear Physics **A415** (1984)189–214

SIGNATURE INVERSION - A FINGERPRINT OF TRIAXIALITY

R. BENGTSSON

NORDITA, Blegdamsvej 17, DK-2100 Copenhagen Ø, Denmark
and
Oak Ridge National Laboratory, Oak Ridge, TN 37830, USA

H. FRISK

Department of Matemathical Physics, Lund Institute of Technology, PO Box 725, S-220 07 Lund 7, Sweden

F. R. MAY

Central Institute for Nuclear Research, Rosendorf, GDR[†]
and
The Niels Bohr Institute, University of Copenhagen, DK-2100 Copenhagen Ø, Denmark

and

J. A. PINSTON

Centre d'Etudes Nucléaires, DRF/Chimie Physique Nucléaire, 85X, F-38041 Grenoble Cedex, France

Received 3 October 1983

Abstract: Theoretical calculations show that the energetic signature splitting of the lowest high-j quasiparticle orbitals can be inverted compared to what is expected for purely prolate ($\gamma = 0°$) or oblate ($\gamma = -60°$) rotational bands, if the nucleus has a triaxial shape with $-120° < \gamma < -60°$ or $0° < \gamma < 60°$. The signature inversion occurs only in certain frequency intervals and for certain positions of the Fermi surface, which can be predicted theoretically. A comparison with experimental data shows that signature inversion has been observed in the predicted regions. From the experimental signature splitting of the $[i_{\frac{13}{2}}]_n$ $[h_{\frac{11}{2}}]_p$ band in the $N = 89$ and $N = 91$ isotones of the rare-earth nuclei, we have deduced the most likely deformations. We find in all cases triaxial deformations with γ-values in the interval $5° < \gamma < 25°$.

1. Introduction

Although many rotational bands in nuclei form regular sequences of states which differ by only one unit in angular momentum ($\Delta I = \hbar$), it is in general more suitable to classify rotational bands also with respect to their signature,

[†] Permanent address.

$\alpha(I = \alpha \bmod 2)$ [ref. [1])]. A rotational band with a given signature then consists of a sequence of states with $\Delta I = 2\hbar$.

Two bands which differ only with respect to the signature may together form either a regular $\Delta I = \hbar$ rotational band or the two signatures may be displayed in energy. In the latter case one could speak of a favoured band, being lowest in energy, and an unfavoured band. The difference in energy can be traced back to the splitting of the quasiparticle trajectories with increasing rotational frequency. Particularly large signature splittings are found for the lowest levels in a high-j shell. This rule has already been pointed out by Stephens [2]) and Meyer-ter-Vehn [3]). Analyses of experimental rotational bands in odd nuclei show that in a given j-shell one and the same signature is always connected with the favoured band. (This signature is for an $i_{13/2}$ shell $\alpha = \frac{1}{2}$ and for an $h_{11/2}$ shell $\alpha = -\frac{1}{2}$.) This behaviour is also predicted from cranked-shell-model calculations, provided a prolate shape of the nucleus is assumed. Recent experimental information on odd-odd nuclei (see sect. 5 for details) shows however that what we normally call the unfavoured signature may under certain circumstances be the one that lies lowest in energy. We shall refer to this situation as *signature inversion* [4]). In order to understand the

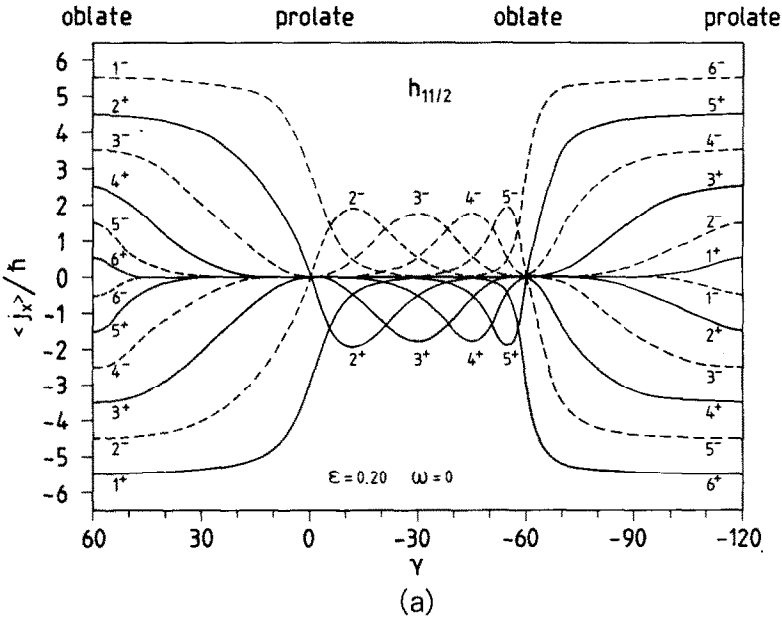

Fig. 1a. Expectation values of the angular momentum component along the x-axis as a function of the γ-deformation for the $h_{11/2}$ single-proton orbitals in a non-rotating deformed potential. The orbitals are numbered by order of increasing energy ($\nu = 1, 2, \ldots, 6$). The x-axis is the symmetry axis for $\gamma = 60°$ and $-120°$ and a perpendicular axis for $\gamma = 0°$ and $-60°$. The linear combination of doubly degenerate orbitals which corresponds to the signature $\alpha = \frac{1}{2}$ is shown by full lines (ν^+). The combination which corresponds to $\alpha = -\frac{1}{2}$ and can be obtained by reflexion through $\langle j_x \rangle = 0$ is shown by dashed lines (ν^-).

general conditions for getting a signature inversion, we shall in the next section discuss the angular momentum properties of a high-j shell. Then we shall establish the general conditions for signature inversion (sect. 3) and predict in which nuclei a signature inversion can be expected (sect. 4), provided γ-deformations are the responsible mechanism for the effect. A survey of the available experimental data will be given in sect. 5. The method of the theoretical calculations will be given in sect. 6 and in sect. 7 we shall investigate what the experimentally observed examples can tell us about the deformation of the nucleus. Finally a comparison between the signature inversion frequency and the backbending frequency will be made.

2. The angular momentum properties of a high-j shell

Since most of the present experimental information about signature inversion concerns the $h_{11/2}$ subshell, we shall base our discussion on this shell. The conclusions can, however, be applied to any high-j shell.

The expectation value of j_x for the single-particle trajectories of the $h_{11/2}$ shell is shown in fig. 1a ($\omega/\omega_0 = 0$) and fig. 1b ($\omega/\omega_0 = 0.04$) as a function of the deformation parameter γ describing the triaxiality of the nucleus. This convenient

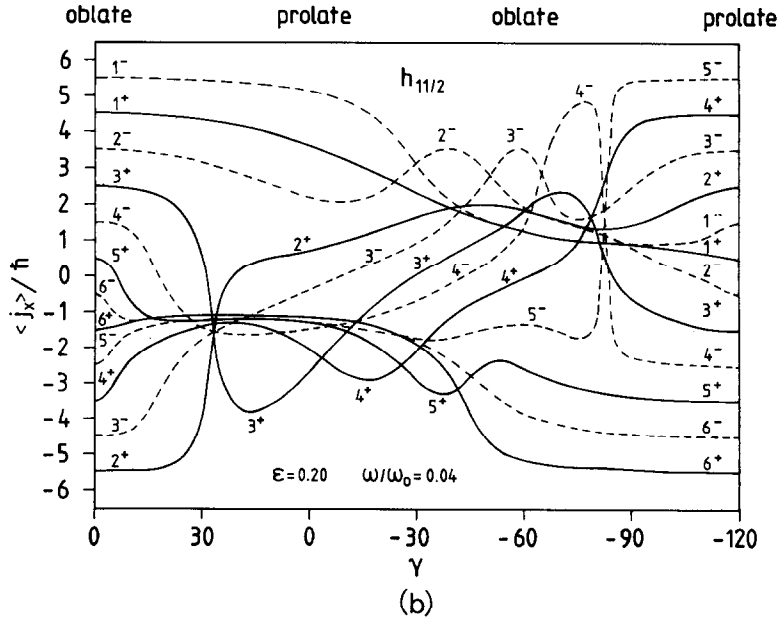

Fig. 1b. Same as fig. 1a, but for $h_{11/2}$ single-proton orbitals in a rotating deformed potential at a frequency $\omega/\omega_0 = 0.04$. Note that the reflection symmetry with respect to the line $\langle j_x \rangle = 0$ is lost.

way of representing $\langle j_x \rangle$ has previously been used by Larsson *et al.* [5]). For $\gamma = 60°$ the nucleus rotates around the oblate symmetry axis and for $\gamma = -120°$ around the prolate symmetry axis. For $\gamma = 0°$ (prolate shape) and for $\gamma = -60°$ (oblate shape) the nucleus has a collective rotation. Although no collective rotation can take place for $\gamma = 60°$ it is very useful to investigate the quasiparticle trajectories at this deformation. Fig. 2 shows three situations corresponding to different positions of the Fermi surface. In the first case (a), when the Fermi surface lies on top of the $K = \frac{11}{2}$ level, we recognize the situation which is familiar from collective $h_{\frac{11}{2}}$ bands in prolate nuclei. The lowest level (orginating from above the Fermi surface at $\omega = 0$) has $\alpha = -\frac{1}{2}$ and the second lowest has $\alpha - \frac{1}{2}$ independent of the rotational frequency (the thick lines in fig. 2). In the two other cases (b, c) there is an interval ($0 < \omega/\omega_0 < \omega_i$ and $\omega_i' < \omega/\omega_0 < \omega_i$, respectively) where the lowest level has

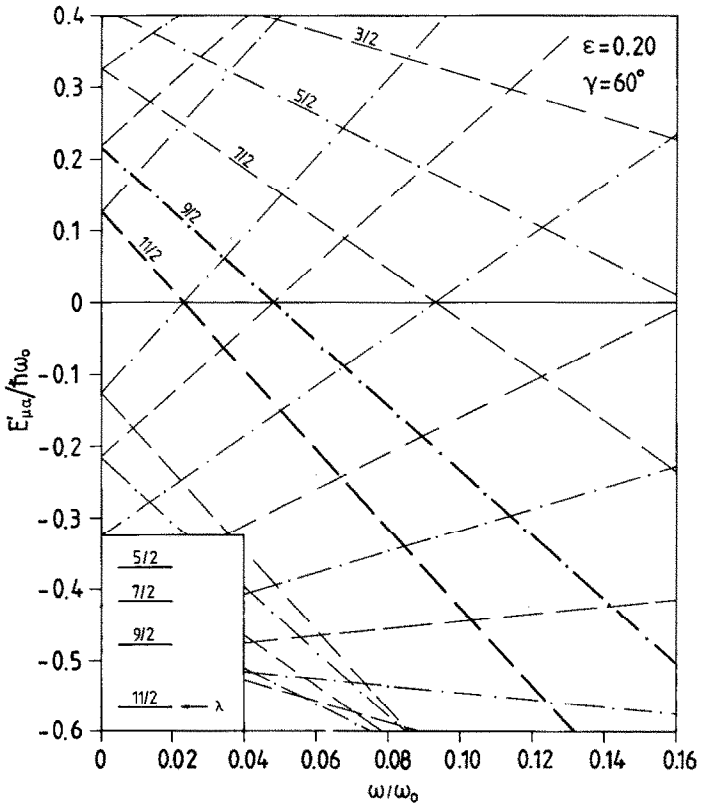

Fig. 2a. Oblate $h_{11/2}$ quasiproton levels as a function of frequency ω/ω_0. Dashed lines corresponds to orbitals with the signature $\alpha = -\frac{1}{2}$, while dashed-dotted ones correspond to orbitals with $\alpha = \frac{1}{2}$. The lowest orbitals of each signature, originating from above the Fermi surface at $\omega = 0$, are shown by thick lines. The position of the Fermi surface, which is here on top of the $K = \frac{11}{2}$ level, is indicated in the lower left corner.

$\alpha = \frac{1}{2}$, which means that there is a signature inversion. Since the quasiparticle trajectories form straight lines for $\gamma = 60°$ (also for $\gamma = -120°$) it is a trivial task to find out what will happen for other positions of the Fermi surface. What we must remember is that at sufficiently high frequencies ($\omega/\omega_0 > \omega_i$) the "favoured" signature is always the lowest one. Below ω_i there may occur other crossings like ω_i' in fig. 2c. These crossings fall, however, beyond the scope of the present investigation.

Turning back to fig. 1a, we see that the oblate ($\gamma = 60°$) pattern persists far out in the γ-plane, in particular for the lowest members of the shell. Already at $\gamma = 10°$ the three lowest pairs of states have $\langle j_x \rangle$ values, which are clearly different from zero at $\omega = 0$. At higher frequencies the aligned states (i.e. those with $\langle j_x \rangle$ clearly > 0) get values of $\langle j_x \rangle$ which approach the limiting oblate values in the whole region, $\gamma > 0$ (fig. 1b). We may therefore expect that the structure of the quasiparticle energies, if plotted versus the rotational frequency, will show clear similarities with the oblate situation also at small positive γ-values provided the

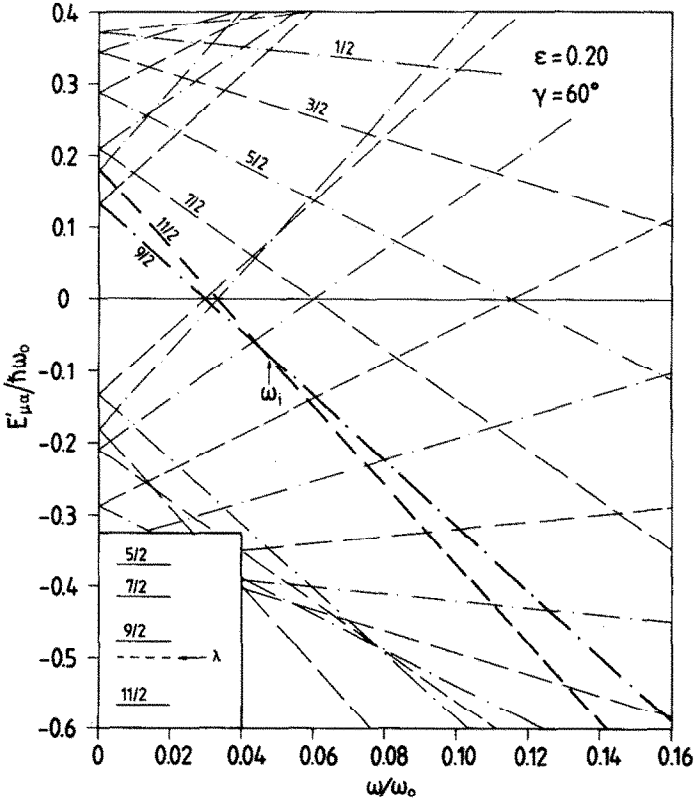

Fig. 2b. Same as fig. 2a, but with the Fermi surface placed slightly below the $K = \frac{9}{2}$ level. The arrow marks the signature inversion frequency ω_i.

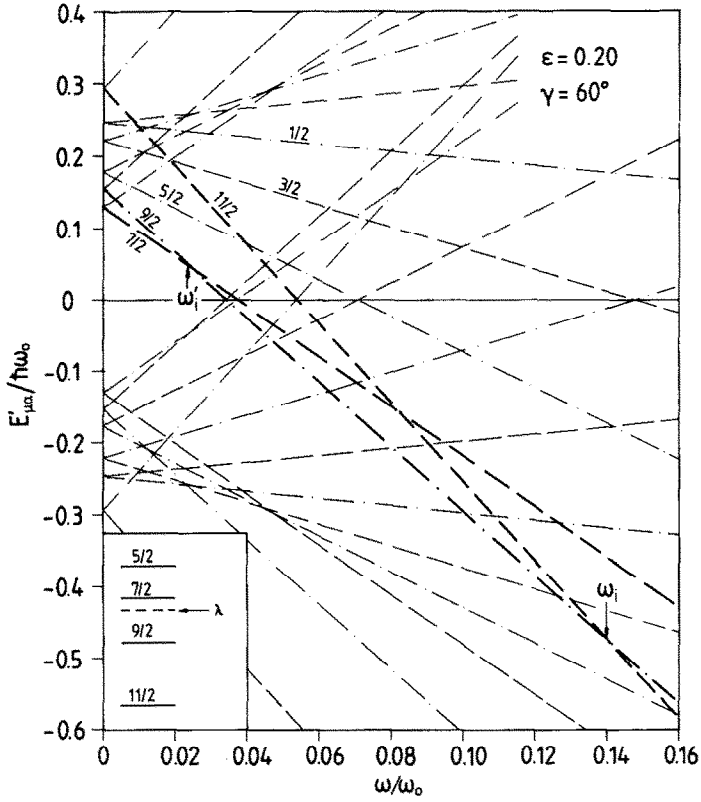

Fig. 2c. Same as fig. 2a, but with the Fermi surface placed slightly below the $K = \frac{7}{2}$ level. Note the appearance of two signature inversion frequencies, ω_i' and ω_i.

Fermi surface lies at a comparable position. That this actually is the case is shown in fig. 3, which shows the quasiparticle levels at $\gamma = 13.5°$. If the interaction between the levels is disregarded, as illustrated by the solid and dotted lines (diabatic levels) in fig. 3a, we can easily see how the aligned, i.e. downsloping, levels originating from the $K = \frac{1}{2}$ and $K = \frac{3}{2}$ states proceed downwards and cross each other in a similar way to that in fig. 2c. In both figures the Fermi energy lies close to the third lowest level of the shell. This is the important point, not the K quantum numbers, which of course must be different in the oblate and near-prolate case. We can also identify the crossing ω_i', in fig. 3a. The main difference compared to the oblate case is due to the non-zero interaction between the levels. The aligned levels will therefore gradually gain angular momentum with increasing rotational frequency and do therefore no longer form straight lines. Another difference is that the lower states of the shell are more compressed in energy, for near-prolate deformations. This is particularly important, since it brings down the crossing frequency ω_i to a frequency region where it can be observed experimentally.

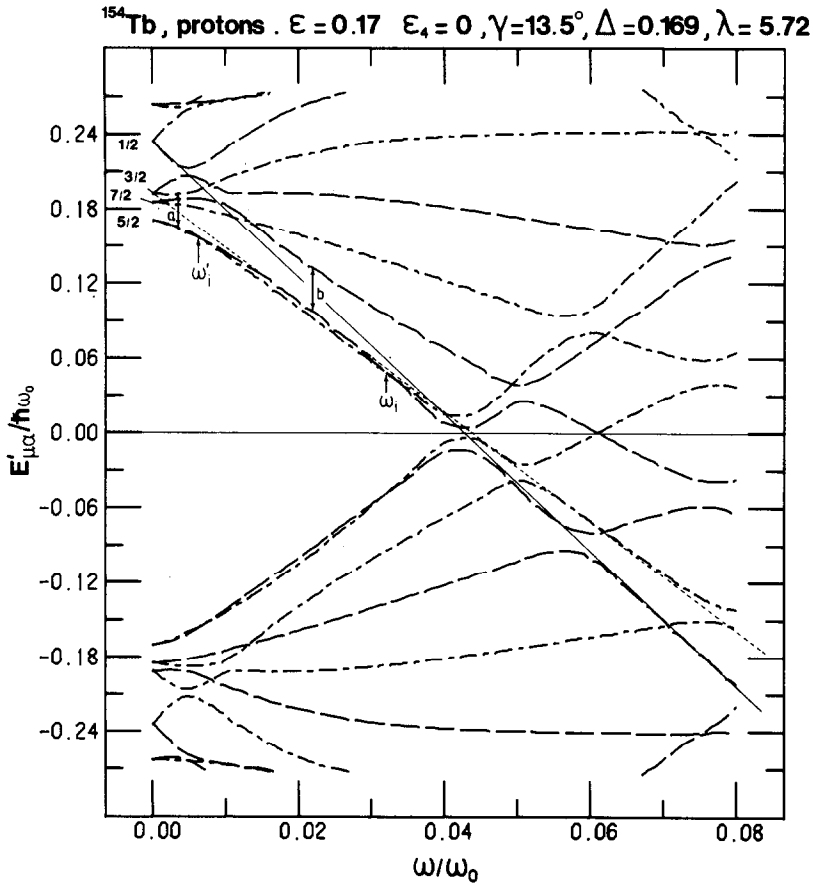

Fig. 3a. Quasiproton orbitals originating from the $h_{11/2}$ shell as functions of the frequency ω/ω_0 at a slightly positive γ-deformation of 13.5°. The notation of lines is the same as in fig. 2a. The pairing gap Δ corresponds to the full odd-even mass difference [23]), while the Fermi surface λ is fixed to give the correct particle number at $\omega/\omega_0 = 0$. The values of Δ and λ indicated in the headline are in units $\hbar\omega_0$. The arrows indicate the frequencies ω_i' and ω_i at which the order of the two lowest orbitals is inverted. The arrows a and b indicate important interactions. The quantum numbers put on the levels at $\omega = 0$ serves only as labels ($\frac{1}{2}$ for the lowest single-particle state, $\frac{3}{2}$ for the second lowest, and so on). Since the deformation is near-prolate they may in practice be thought of as K quantum numbers, although the actual wave functions are mixtures of different K-values also at $\omega = 0$.

3. General conditions for signature inversion

We can now specify the necessary conditions for the occurence of a signature inversion in collective rotational bands with *near-prolate deformation*, caused by the particular structure of the high-j levels.

(i) The deformation must be triaxial with $\gamma > 0$. This assures that there are states

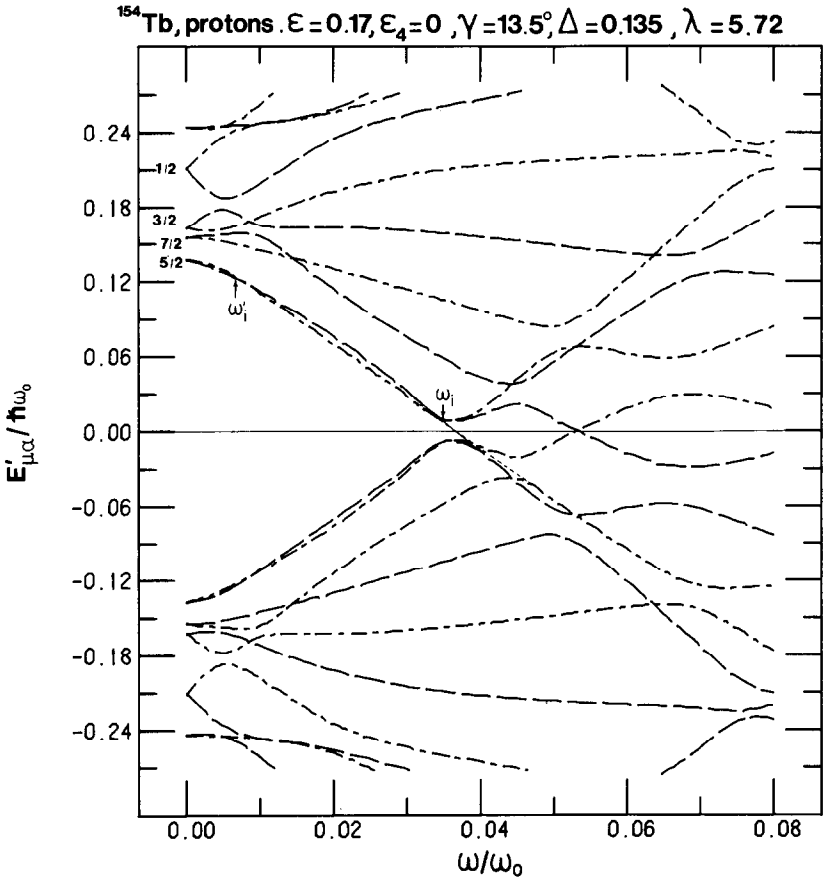

Fig. 3b. Same as fig. 3a, but with the pairing gap corresponding to a reduced odd-even mass difference, $\Delta = 0.8\Delta_{o.e.}$.

(in practice the $K = \frac{3}{2}$ state) which at $\omega = 0$ split up in such a way that what is normally called the unfavoured signature slopes down (cf. fig. 3a). For $\gamma < 0$ the favoured signature is the downsloping one, i.e. has $\langle j_x \rangle > 0$, for all states (cf. fig. 1a). This leads to an increase of the normal (prolate) signature splitting.

(ii) The $K = \frac{3}{2}$ level must lie closer to the Fermi surface than the $K = \frac{1}{2}$ level. Otherwise the inverted order of the signatures will not be seen in the lowest pair of quasiparticle states (cf. figs. 3a–c). Experimentally it is in most cases not possible to get any information about the signature splitting at frequencies $\lesssim 100$ keV [cf. refs. [6–8]) and figs. 4–5]. A position of the Fermi surface between the $K = \frac{3}{2}$ and the $K = \frac{5}{2}$ levels, or higher, is therefore required. This guarantees a high enough inversion frequency for the experimental detection of the signature inversion. If, on the other hand, the Fermi surface lies too high the signature splitting of the lowest

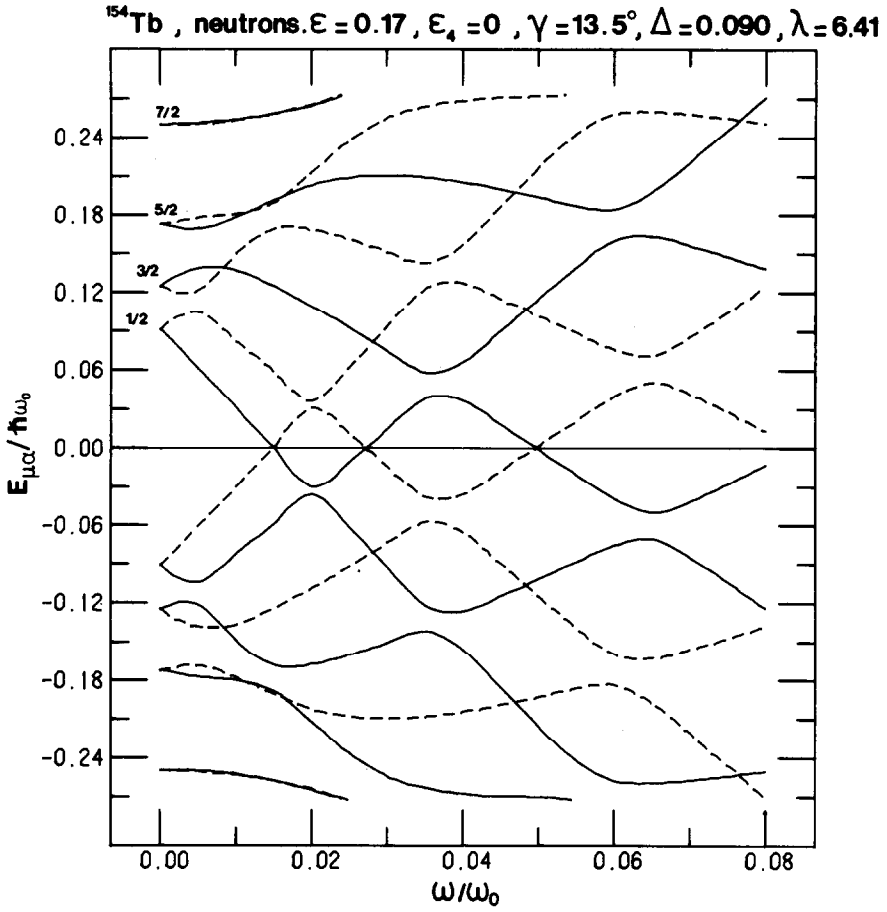

Fig. 3c. Same as fig. 3a, but for the $i_{13/2}$ quasineutron orbitals. Full lines correspond to orbitals with the signature $\alpha = \frac{1}{2}$, and dashed ones to orbitals with $\alpha = -\frac{1}{2}$. A reduced pairing gap, $\Delta = 0.8\Delta_{\text{o.e.}}$, has been used.

quasiparticle levels becomes very small. We can therefore conclude that the experimental detection of a significant signature inversion requires that the Fermi surface lies in the vicinity of the $K = \frac{5}{2}$ or $\frac{7}{2}$ levels.

It should finally be noted that signature inversion also may occur when a *near-oblate nucleus* rotates collectively ($\gamma \approx -60°$). In this case, however, the Fermi surface must lie in the upper part of the shell. This can immediately be realized from fig. 1 by comparing the interval $-120° < \gamma < -60°$ with the interval $0° < \gamma < 60°$. In a recent investigation of classical orbits by Hamamoto and Mottelson [9]), based on a cranking hamiltonian acting within a pure $i_{13/2}$ quasineutron shell, these new features seen in the quantal spectra have been well established.

4. In which nuclei can we expect to see a signature inversion?

From the previous section we may conclude that a signature inversion will only be seen in nuclei which are sufficiently soft to γ-deformations, since then the alignment of one or a few quasiparticles will be enough for polarizing the core and thereby establish a triaxial deformation. This has recently been demonstrated by Frauendorf and May who studied total routhians derived within a triaxial cranked shell model [10]. Such nuclei are in general to be found near the edges of the deformed regions. In the rare-earth region this applies to nuclei with neutron numbers close to 90 and proton numbers $62 < Z < 70$. In these nuclei the *neutron Fermi surface* lies in the vicinity of the $K = \frac{1}{2}$ or $\frac{3}{2}$ members of the $i_{\frac{13}{2}}$ shell, which is too low to give a signature inversion of the $i_{\frac{13}{2}}$ neutron levels. It will occur for $N = 93$ provided there is still a triaxial deformation of $\gamma \gtrsim 5°$. However, an inspection of the corresponding quasineutron diagram $E'_{\alpha\mu}(\omega)$ shows that the signature inversion occurs only at very small frequencies (below the detectable range) due to a still too low Fermi surface. At $N = 95$ the nuclei are no longer very γ-soft and a triaxial deformation is unlikely. In the *proton system* the Fermi surface lies close to the $K = \frac{5}{2}$ member of the $h_{\frac{11}{2}}$ shell in Eu and Tb and close to the $K = \frac{7}{2}$ level in Ho and Tm. A signature inversion of the $h_{\frac{11}{2}}$ proton levels can therefore be expected, provided that $\gamma > 0$. For further details see sect. 5.

In the actinide region the corresponding transition from spherical to deformed shapes occurs for neutron numbers in the range $130 < N < 135$. As in the rare-earth region these neutron numbers are too low to give a signature inversion of the neutron levels (in this case those of the $j_{\frac{15}{2}}$ shell). In the proton system an inversion of the $i_{\frac{13}{2}}$ levels is expected for proton numbers > 93. Combining these proton numbers with the transitional neutron numbers leads to very neutron deficient isotopes, out of reach of experimental investigations.

In lighter nuclei an inversion of the $g_{\frac{9}{2}}$ levels can be expected for proton as well as neutron numbers between 39 and 47, if a near-prolate shape is assumed. Several γ-soft nuclei in the $A \approx 80$ mass region have these neutron numbers, while γ-soft nuclei with the corresponding proton numbers may as well be found in the $A \approx 100$ mass region.

Significant oblate deformations are comparatively rare, in the heavier mass regions. One exception is the Pt-Hg region, where oblate shapes are expected to dominate, at least for $N \geqq 110$. These nuclei are also very γ-soft as they lie in the transitional region below the $Z = 82$ and $N = 126$ gaps [cf. ref. [11])]. For neutron numbers around 110, the neutron Fermi surface lies at the right position in the upper part of the $i_{\frac{13}{2}}$ shell for producing a signature inversion provided that $-90° < \gamma < -60°$. In the $A \approx 80$ and $A \approx 100$ mass regions it can be expected that a number of nuclei have near-oblate shapes [12]). A signature inversion (of the $g_{\frac{9}{2}}$ levels) can be expected also in these nuclei, most likely for particle numbers 41 and 43.

The theoretical calculations show that signature inversion can also occur in other shells than the high-j shells. Since those shells lie much closer in energy they also mix considerably at small deformations. The particular features in the quasiparticle level spectrum caused by triaxial deformations are therefore less clean and partly hidden by the overall interaction between levels originating from different j-shells.

5. Experimental information about signature inversion

An inspection of the available experimental data shows that signature inversion has never been observed in the high-j bands of odd-A nuclei [see e.g. ref. [8])]. The reason for this seems to be very simple. The one-quasiparticle configurations, which are most favourable for creating triaxial deformations with $\gamma > 0$, are those which involve the lowest states of a high-j shell [see refs. [10, 13])] but according to the previous section, the position of the Fermi surface is then too low for getting a signature inversion. To get an inversion the odd particle must be placed at a higher position in the shell, in an orbital originating from the $K = \frac{5}{2}$ or $\frac{7}{2}$ levels. Such configurations are not expected to produce triaxial deformations with $\gamma > 0$ [refs. [10, 13])]. If triaxial deformations occur, they will rather have $\gamma < 0$, which means that also in this case there will be no signature inversion.

To find examples of signature inversion one has to go to configurations containing more than one excited quasiparticle. The best cases turn out to be the yrast bands of odd-odd nuclei, which, except for the lowest spins, in general correspond to a configuration with one aligned high-j neutron and one aligned high-j proton. This is the case for a number of odd-odd rare-earth nuclei with neutron number around 90, in which the yrast band has the configuration $[i_{13/2}]_n$ $[h_{11/2}]_p$. Here the neutron Fermi surface lies close to the $K = \frac{1}{2}$ level of the $i_{13/2}$ shell and consequently, as outlined at the beginning of this section, the odd neutron has a strong polarizing effect on the nucleus, which results in a triaxial shape with $\gamma > 0$. The proton Fermi surface is placed at a higher position in the $h_{11/2}$ shell (cf. sect. 4). Since the driving force of the odd proton is considerably weaker than that of the odd neutron [10, 13]) the odd proton will not influence very much the deformation of the nucleus. We may then expect that due to the triaxial deformation created by the presence of the odd neutron, i.e. $\gamma > 0$, a signature inversion of the lowest proton orbitals may occur.

In the neutron system the signature splitting is very large and the $\alpha = \frac{1}{2}$ signature is strongly favoured energetically (cf. fig. 3c). The signature inversion should therefore show up when comparing the configuration $[i_{13/2}; \alpha = \frac{1}{2}]_n$ $[h_{11/2}; \alpha = -\frac{1}{2}]_p$ and $[i_{13/2}; \alpha = \frac{1}{2}]_n$ $[h_{11/2}; \alpha = \frac{1}{2}]_p$. This is done in fig. 4a, which shows the experimental routhians of ^{154}Tb. It is clearly seen that the two signatures cross each other at $\hbar\omega \approx 0.27$ MeV. Below this frequency the $\alpha = 1$ signature is lowest,

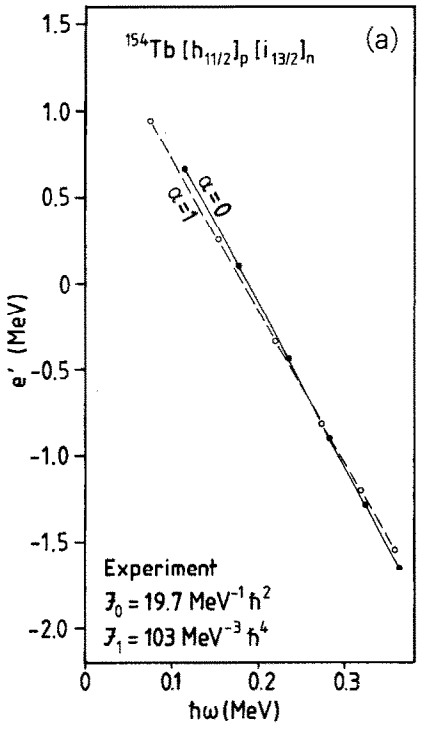

Fig. 4a. Experimental routhians for the configuration $[h_{11/2};\alpha=\pm\frac{1}{2}]_p$ $[i_{13/2};\alpha=\frac{1}{2}]_n$ in ^{154}Tb. The routhians are relative to a reference [22]) defined by the parameters in the lower left corner. The position of the experimental routhians is arbitrarily chosen, because the band-head energy is not known [7]). Signature inversion occurs at $\hbar\omega \approx 0.27$ MeV.

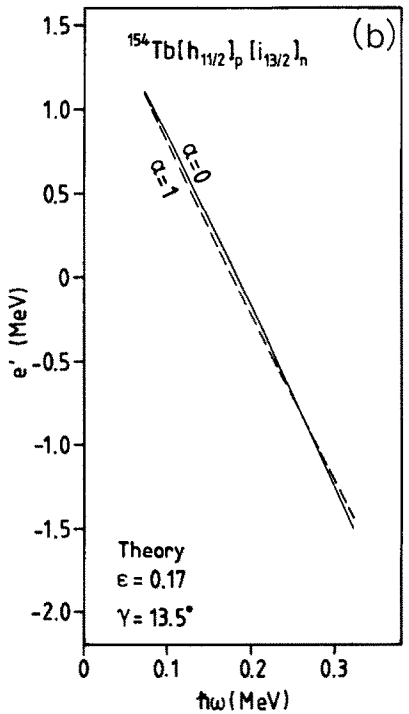

Fig. 4b. Same as fig. 4a, but calculated routhians. The routhians are constructed from the appropriate orbitals of figs. 3b and 3c. The signature inversion is well described at the slightly positive γ-deformation 13.5°.

which implies that the $[h_{\frac{11}{2}};\alpha=\frac{1}{2}]_p$ level must lie below the $[h_{\frac{11}{2}};\alpha=-\frac{1}{2}]_p$ level, i.e. the two signatures lie in inverted order compared to what is expected for a pure prolate shape.

The energy splitting between the two signatures is not very large. To magnify the splitting we have instead plotted the energy difference between the routhians, $E'(\alpha=1)-E'(\alpha=0)$, in fig. 5a (for $N=89$) and fig. 5b (for $N=91$). A negative energy thus means that the signatures are inverted. Fig. 5 includes all $N=89$ and $N=91$ isotones for which a signature inversion has been established experimentally. It is obvious that the data show a number of regular features. Thus the inversion frequency increases with the proton number for both the $N=89$ and $N=91$ isotones. Furthermore the inversion frequency is for a given proton number always larger for $N=89$ than for $N=91$. The largest observed negative

energy splitting (fig. 5) is for $N = 89$ between 50 and 75 keV depending on the proton number, while it is only between 10 and 35 keV for $N = 91$. Signature inversion has also been observed in the $N = 93$ isotones ^{160}Ho($\omega_i = 0.19$ MeV) [ref. [14])] and ^{162}Tm ($\omega_i = 0.25$ MeV) [ref. [15])] where the maximal negative signature splitting is -2 keV and -9 keV, respectively, which fits well into the general pattern of the data shown in fig. 5.

Signature inversion has also been observed in other mass regions. One example is given by the gold isotopes ^{188,190}Au [ref. [16])]. The configuration assignment is the same as before, i.e. $[i_{13/2}]_n\,[h_{11/2}]_p$, but in contrast to the $N = 90$ region the shape of the nucleus is near-oblate and the signature inversion is caused by the odd neutron, which may be placed in either the $[i_{13/2}; \alpha = \frac{1}{2}]$ or $[i_{13/2}; \alpha = -\frac{1}{2}]$ level while the odd proton for energetic reasons must be assumed to occupy the $[h_{11/2}; \alpha = -\frac{1}{2}]$ level.

Another example is provided by the isotopes ^{74,76}Br [refs. [17,18])], which both

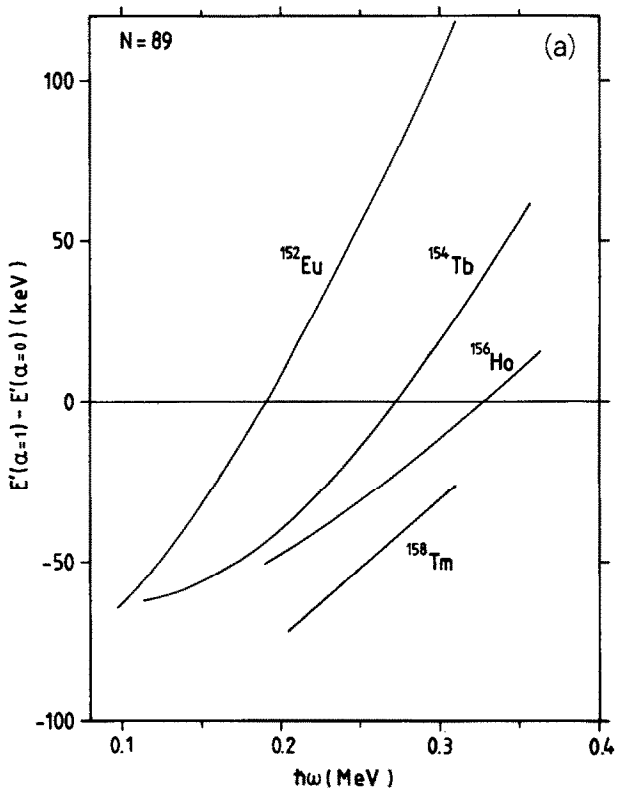

Fig. 5a. Experimental energetic signature splittings as function of the rotational frequency $\hbar\omega$ in ^{152}Eu [ref. [6])], ^{154}Tb [ref. [7])], ^{156}Ho [ref. [30])] and ^{158}Tm [ref. [29])]. The band corresponding to $\alpha = 1$ is the lower one if $E'(\alpha = 1) - E'(\alpha = 0)$ is negative. The signature inversion frequencies are given by the intersections with the line $E'(\alpha = 1) - E'(\alpha = 0) = 0$.

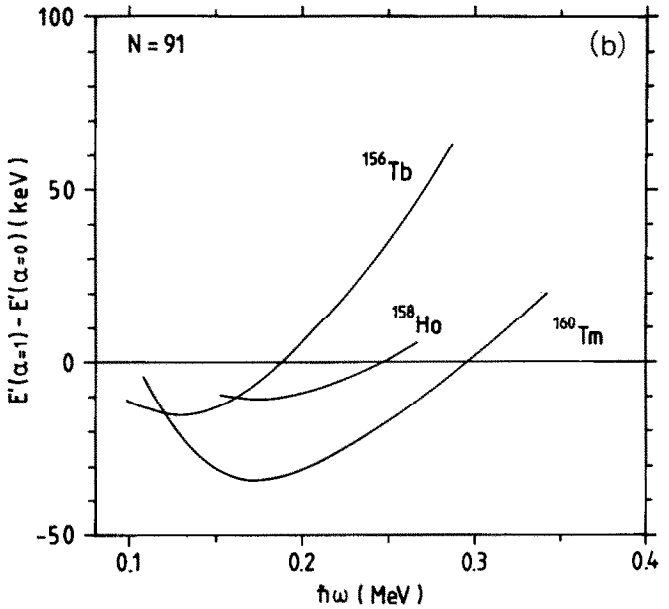

Fig. 5b. Same as fig. 5a, but for the $N = 91$ Tb [ref. [7])], Ho [ref. [31])] and Tm [ref. [14])] isotones.

have the yrast configuration $[g_{\frac{7}{2}}]_n\,[g_{\frac{7}{2}}]_p$. It is hard to determine whether the deformation of these nuclei is mainly prolate or oblate, but it seems easier to understand the data if a near-prolate shape is assumed. The signature inversion must in any case be a neutron effect.

One may also expect that signature inversion may occur in the s-band of odd-even nuclei in configurations like $[i_{13/2};\alpha=\frac{1}{2}]_n\,[i_{13/2};\alpha=-\frac{1}{2}]_n\,[h_{11/2};\alpha=\pm\frac{1}{2}]_p$, where the aligned neutrons could produce a triaxial deformation, which can be detected by comparing the energy of the routhians corresponding to the configurations where the odd proton is placed in the $\alpha=\frac{1}{2}$ and $\alpha=-\frac{1}{2}$ levels, respectively. Experimental data of this kind exist for ^{155,157}Ho [ref. [19])] and ^{159}Tm [ref. [20])]. Below the backbending the $[h_{11/2}]_p$ bands show a signature splitting of normal order, which is best understood if negative γ-values, $\gamma \approx -20°$, are assumed. Above the backbending there is practically no signature splitting, but a closer investigation of the data shows that the signatures are in fact inverted, indicating small positive γ-values. In fact, the signature splitting is expected to be small, since above the backbending frequency we are close to the inversion frequency (cf. figs. 5 and 11).

As already mentioned in sect. 4, we expect that signature inversion will also occur in other shells than the high-j intruder shells. The sidebands AF and AE [see ref. [8])] of even-even nuclei provide us with the possibility to test this prediction. In the rare-earth region, particle A, which is an $i_{13/2}$ quasineutron, will create a triaxial

deformation with $\gamma > 0°$ if the Fermi surface lies in the bottom of the $i_{\frac{13}{2}}$ shell, which is the case for $N \approx 90$. The triaxial deformation thus created should be reflected in the signature splitting of the negative-parity quasineutron levels E and F, which have a mixed $h_{\frac{9}{2}}+f_{\frac{7}{2}}$ character, and for certain positions of the Fermi surface will show signature inversion. An inspection of experimental data [8]) shows that signature inversion indeed occurs. For example the AE and AF bands in ^{160}Yb show signature inversion below $I = 12\hbar$. We shall, however, not discuss these configurations any further, because the negative-parity sidebands are excited configurations, which at low spins ($I \lesssim 15\hbar$) often lie close to, or are even crossed by, other excited bands, like octupole vibrational bands [21]). The interaction with these bands clearly pertubes the signature splitting [21]). The negative-parity sidebands can therefore in general not be used to estimate the deformation of the nucleus based on the signature splitting alone.

6. Theoretical calculations

Theoretical calculations have been made for all nuclei shown in fig. 5. The calculations are based on the cranked shell model described in ref. [22]), extended here to triaxial shapes. We have investigated the quasiparticle routhians (cf. fig. 3) in a part of the (ε, γ) plane ($0.10 \leqq \varepsilon \leqq 0.22$ and $0 \leqq \gamma \leqq 30°$). In the given mass region deformation-energy calculations give only small negative hexadecapole deformations [11]), which are without any significant influence on the occurrence of signature inversion in the quasiparticle diagrams. Therefore we have used $\varepsilon_4 = 0$ throughout our calculations. The main interest has been focused on the lowest excited high-j levels, in particular the $h_{\frac{11}{2}}$ proton levels. The inversion frequency and the signature splitting have been studied as functions of ε and γ. As an example we show the inversion frequency ω_i of ^{154}Tb in fig. 6. It has a very regular behaviour and increases both as a function of ε and γ. In fig. 7 we show the energy splitting between the two signatures at a fixed frequency ($\hbar\omega \approx 150$ keV). Along the prolate axis the signature splitting decreases with increasing ε, which is well known, but we also see that there is a valley in the (ε, γ) plane with negative signature splitting. The negative signature splitting increases rapidly towards the upper left corner of the plot. Positive signature splittings appear in the upper right corner, because at these deformations the frequency used in the plot lies below ω_i' (cf. figs. 3a, b) and therefore the two signatures lie in the normal order.

The calculations are, as in ref. [22]), based on the assumption that a constant value of the pairing gap, Δ, can be used. This has been chosen as 80% of the odd-even mass difference, and has been calculated from the masses of ref. [23]). The reduced values have been used, because of the presence of an excited quasiparticle both in the proton and neutron systems [cf. ref. [22])]. In fig. 4b the theoretical routhians for ^{154}Tb are shown. They correspond to the sum of the appropriate proton (fig. 3b)

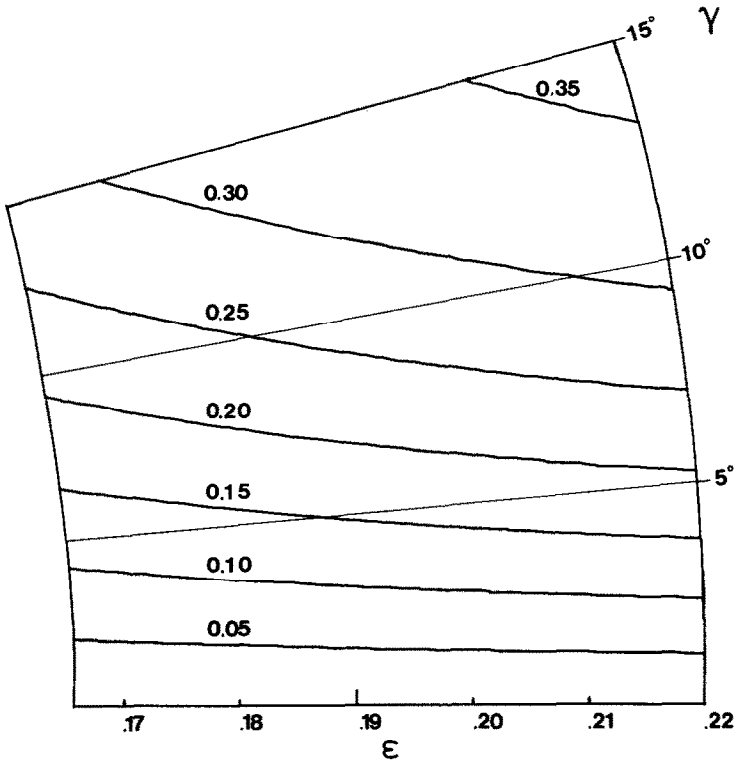

Fig. 6. The deformation dependence (ε, γ) of the signature inversion frequency (in units of MeV) in ^{154}Tb. The Δ-value used is $\Delta = 0.8\Delta_{o.e.}$. The signature inversion frequency increases with both ε and γ.

and neutron (fig. 3c) routhians. A comparison with the experimental routhians in fig. 4a shows that the alignment (i.e. the slope) is quite well described. Since the alignment is strongly dependent on the Δ-value, we taken the agreement as an indication that the Δ-values used are reasonable.

It must be pointed out that the inversion frequency is by no means independent on the choice of Δ. This is clearly seen by comparing figs. 3a and 3b. In fig. 3a Δ is equal to the full odd-even mass difference, while in fig. 3b it is only 80% of it. It is seen that an increase of Δ lowers the inversion frequency. The reason is that a larger Δ leads to a higher compression of the levels above the gap, which means that the $K = \frac{1}{2}$ level comes closer to the $K = \frac{3}{2}$ level and the levels will therefore interact (the arrow b) at a lower frequency, which automatically brings down the inversion frequency. It should be noted that the first backbending frequency behaves in the opposite way. It increases with increasing Δ.

The Δ-dependence of ω_i must be kept in mind when judging the results of the

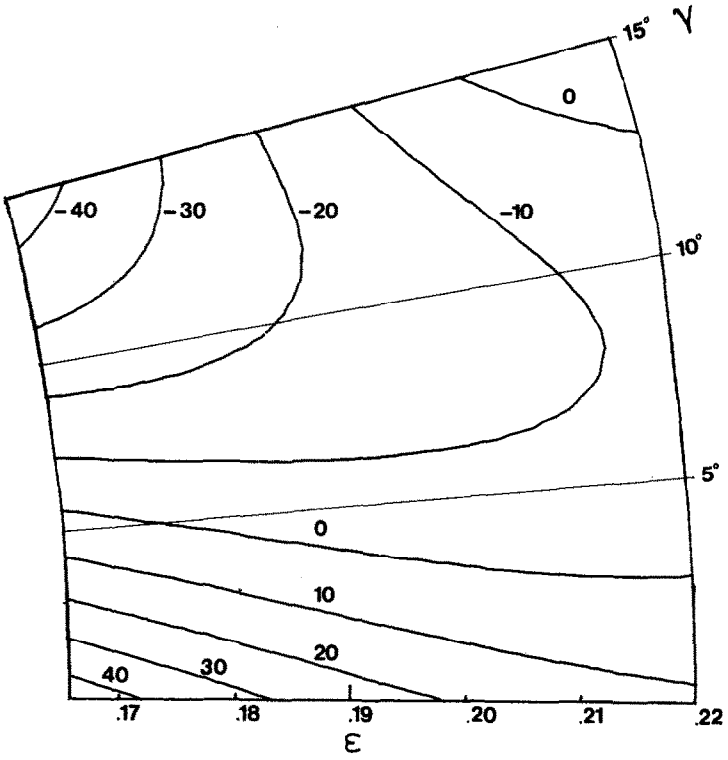

Fig. 7. The deformation dependence (ε, γ) of the signature splitting (in units of keV) in ^{154}Tb at a fixed frequency ($\hbar\omega \approx 150$ keV). Note the valley with negative signature splitting. The same Δ-value as in fig. 6.

next section, since a different assumption about Δ would somewhat modify the results.

7. Estimated deformations for the $N = 89$ and $N = 91$ isotones

The negative signature splitting is in most cases quite small. The largest value observed so far (in ^{158}Tm) is only 72 keV. One can therefore easily imagine alternative explanations, which need not include triaxial deformations. It is for example obvious that the experimental data could as well be explained if one assumes different (if necessary ω-dependent) Δ-values and/or deformations for the two signatures. It is also possible that a residual neutron-proton interaction might explain the signature inversion, or at least a part of it. Such an interaction is

essential for understanding the band-head energies of odd-odd nuclei[24]), but it is not known whether it is of any importance for the strongly aligned configurations of interest here, which do not conserve K as a good quantum number.

In order to make it at all possible to estimate the deformation of a nucleus from the signature splitting of the routhians, we are forced to neglect the possible influence from the kind of effects mentioned above, which means that the subsequent calculations are made under the following assumptions:

(i) The pairing gap and the deformation corresponding to the two signatures are (nearly) equal. Preliminary self-consistent calculations performed for both signatures in ^{152}Eu give no drastic difference neither in the deformation nor in the pairing gaps[25]) of the two signatures.

(ii) The residual neutron-proton interaction does not essentially influence the signature splitting. There exist to our knowledge no investigations, which could give some more precise information about the validity of the above statements. On the other hand, we have at least some indirect evidence that γ-deformations are a very likely explanation of the inverted signature splitting. We can thus conclude from sects. 4 and 5 that signature inversion has been observed in precisely those mass regions and configurations where it is expected to occur, if γ-deformations are the basic explanation, and nowhere else.

It is obvious that the inversion frequency alone is not enough to determine the deformation of a nucleus, because it only tells us that the deformation must lie along a curve in the (ε, γ) plane (cf. fig. 6). We therefore need a second condition to fix the deformation. One possibility would be to find an optimal fit to the experimental signature splitting (fig. 5) over the whole frequency region observed. An attempt along this line shows that it is not always possible to make a reasonable fit. The explanation could be that the deformation is not constant, but changes gradually with increasing rotational frequency. Such deformation changes are known to occur in the $N \approx 90$ region[26]). A better alternative is to restrict the fit to a limited frequency interval (of the order of 50–100 keV) in the vicinity of the inversion frequency. In this case it is more justified to consider the deformation as constant. For practical reasons we have in most cases chosen this frequency interval to lie just below the inversion frequency. Then we can avoid using theoretical data from the first band-crossing region (cf. fig. 3b). Experimentally the first crossing is blocked and will have no influence on the data. A fit of ε and γ along the lines described above gives a quite good accuracy, where the main uncertainty depends on the extention of the frequency interval that is taken into consideration.

When the theoretical signature splitting, calculated at the fitted deformations, is compared to experiment over the whole experimentally known frequency region, it is found that the agreement differs a lot depending on the nucleus. In some cases, like ^{152}Eu (fig. 8a), the discrepancy in the signature splitting never exceeds 15 keV, although only a small frequency interval below ω_i was used to fit ε and γ. In other

cases, like ^{156}Tb (fig. 8b), it is not possible to get a good agreement with the experimental data at all frequencies using just one set of ε and γ. We see in both figs. 8a and 8b that the theory overestimates the signature splitting at high frequencies. A better agreement would be obtained if it was taken into account that Δ is not constant but decreases slowly with ω, since a smaller Δ decreases the signature splitting. A similar improvement can be obtained if one assumes that the deformation depends on ω, as illustrated in fig. 8b. This figure also shows that the necessary deformation change is an increase of ε and to some extent a decrease of γ as the frequency increases. Similar conclusions can be drawn for other nuclei. We have not found any particular correlation between the magnitude of the fitted deformation parameters and the agreement with experiment. The nuclei shown in fig. 8 are the two most deformed ones.

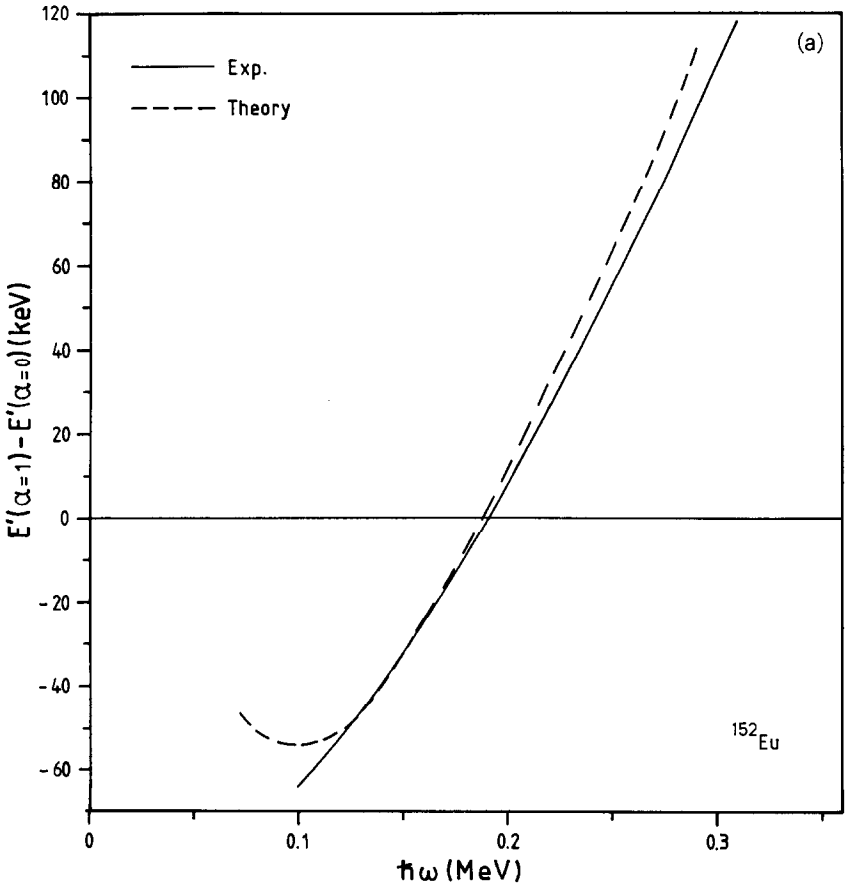

Fig. 8a. Comparison between the calculated and the experimental[6]) signature splitting in ^{152}Eu. The theoretical curve is calculated at the deformation determined in sect. 7, $\varepsilon = 0.188$ and $\gamma = 10.7°$.

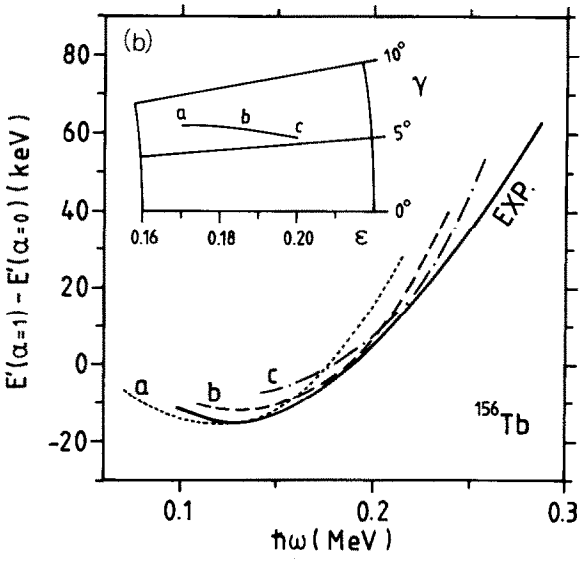

Fig. 8b. Same as fig. 8a but for ^{156}Tb. Three different deformations are used. The theoretical curves fit the experimental one[7]) only within limited frequency intervals.

In fig. 9 we have summarized the deformations that have been estimated for the $[i_{\frac{13}{2}}]_n$ $[h_{\frac{11}{2}}]_p$ bands of the odd-odd $N = 89$ and $N = 91$ isotones, based on the signature splitting. The exact values are somewhat dependent on the specific assumptions made, as discussed above. It could at this point be mentioned that when we estimated the deformations, requiring that ω_i and the largest observed negative signature splitting (for $N = 89$ that at the lowest observed frequency, for $N = 91$ that at the minimum point, cf. fig. 5) were correctly reproduced we found practically the same parameter values as shown in fig. 9 (the largest discrepancy was 0.008 in ε and 1.5° in γ). In fact, figs. 6 and 7 can be used to make a reasonable estimate of ε and γ. By putting the two figures on top of each other one easily finds the deformation point which gives both the right inversion frequency and signature splitting. For ^{154}Tb, for which the figures are drawn, this point happens to lie just outside the upper left corner of the plot. (Note that the figs. 6 and 7 only show a part of the investigated deformation space, cf. sect. 6.) However, the corresponding plots of the inversion frequency and the signature splitting for ^{156}Tb are very similar, and figs. 6 and 7 can therefore also be used to estimate the deformation of this nucleus. From fig. 5b we see that the inversion frequency of ^{156}Tb is 0.19 MeV and that the signature splitting at $\hbar\omega = 0.15$ MeV (the frequency used in fig. 7) is about -13 keV. Requiring that these two quantities should both be reproduced at the same deformation, we find that $\varepsilon \approx 0.18$ and $\gamma \approx 7°$, which is essentially the same deformation as the one shown in fig. 9. We therefore dare to draw the following qualitative conclusions from fig. 9, which should be independent of the

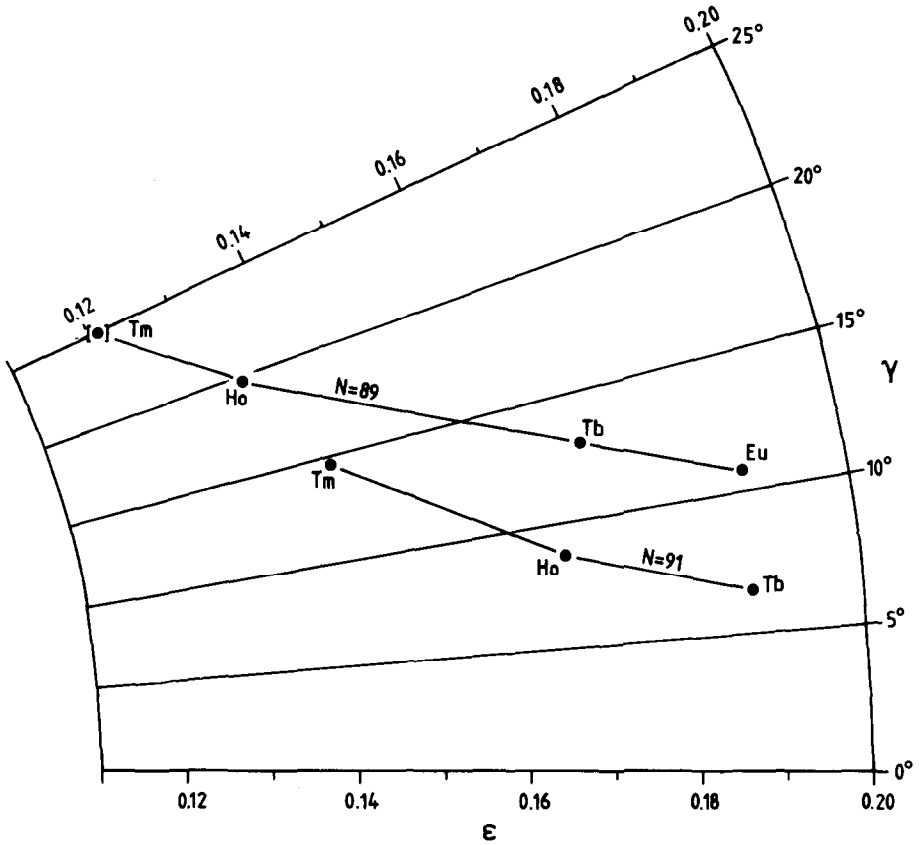

Fig. 9. A summary of the deformations of the $[h_{11/2}]_p$ $[i_{13/2}]_n$ bands of the $N = 89$ and $N = 91$ isotones, estimated in accordance with the principles outlined in sect. 7.

computational details:

(i) All the considered nuclei have a triaxial deformation with $\gamma > 0$.

(ii) For a given proton number, γ is larger and ε smaller for $N = 89$ than for $N = 91$.

(iii) Within each isotone chain γ increases and ε decreases with increasing proton number.

These findings are by no means surprising, when compared to what we know about the ground-state deformations and potential energy surfaces of the near-lying even-even nuclei[11, 26, 27]). The only surprising thing is the comparatively small ε-values which occur, in particular, for some of the heavier nuclei.

In an attempt to find out how reasonable the deformations are we calculated the energy, E, as a function of the spin, I, using the deformations of fig. 9 and a constant $\Delta = 0.8\Delta_{o.e.}$, i.e. the same as used for calculating the routhians. The

agreement with experiment is quite satisfactory for the $N = 89$ isotones as illustrated in fig. 10 for ^{152}Eu. This means that the computed deformations have a sufficient collectivity to account for the experimentally observed moment of inertia, i.e. the curvature in fig. 10. The agreement is worse for the $N = 91$ isotones. In fact the discrepancy is much larger than observed in any calculations of this kind [26, 28]). A striking discrepancy is also observed in the alignment of the $N = 91$ isotones,

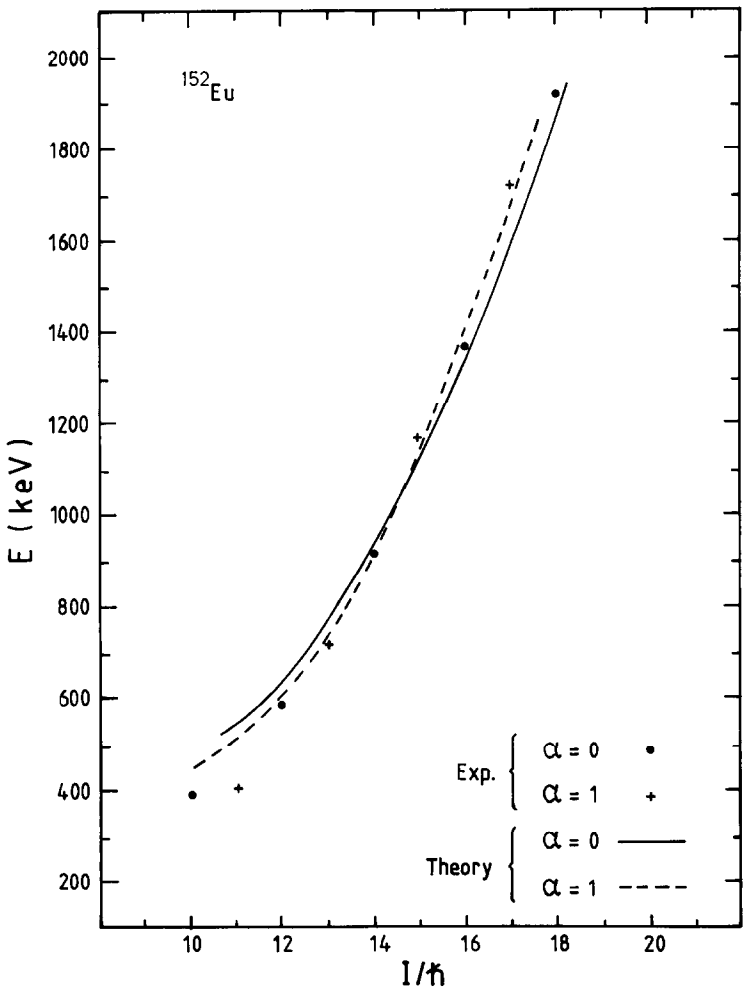

Fig. 10. The energy (E) as a function of spin (I) for the configurations $[h_{11/2}; \alpha = \pm\frac{1}{2}]_p$ $[i_{13/2}; \alpha = \frac{1}{2}]_n$ in ^{152}Eu. The theoretical curves are calculated using the estimated deformation: $\varepsilon = 0.188$, $\gamma = 10.7°$ and constant pairing gaps, $\Delta = 0.8\Delta_{o.e.}$ for both protons and neutrons. The experimental curvature, i.e. the moment of inertia, is reasonably well reproduced. The zero point of the energy scale is arbitrarily chosen, and the relative position of the theoretical curves and the experimental points has been adjusted to simplify a comparison.

where the experimental alignment is about $2\hbar$ smaller than calculated. These observations have led us to suspect that the experimental spin assignments for the $[i_{13/2}]_n$ $[h_{11/2}]_p$ bands of the $N = 91$ isotones may be systematically 2 units too low. Increasing the experimental spins by $2\hbar$ does not only give an agreement between the theoretical and experimental alignments. It also gives a much more reasonable agreement for the $E(I)$ plots. Furthermore, a comparison of the experimental rotational (or transition) energies within the various isotope chains shows an irregularity at $N = 91$, which is removed if the experimental spin values are increased. For these reasons we find a reevaluation of the experimental spin assignments to be highly desirable.

The analyses made in this paper are based on the rotational frequencies, not on the spin values. It is therefore practically independent on the experimental spin assignments. A weak spin dependence enters, however, due to the assumption of a non-zero K-value in the calculation of the experimental rotational frequencies [see ref. [22])], but it will hardly effect the estimated deformations.

8. Signature inversion and backbending frequencies

The signature inversion frequency is compared to the various observed backbending frequencies in fig. 11. Compared to the inversion frequency, which increases rapidly with the proton number and decreases with the neutron number, the backbending frequencies are very little dependent on the nucleon number. Thus in ^{152}Eu, ^{154,156}Tb and ^{158}Ho the inversion frequency is smaller than or roughly equal to the first (neutron) backbending frequency, ω_1(n), while for the remaining nuclei it is clearly larger. It is therefore likely that a signature inversion in the s-band of odd-even nuclei, $[i_{13/2}; \alpha = \frac{1}{2}]_n$ $[i_{13/2}; \alpha = -\frac{1}{2}]_n$ $[h_{11/2}; \alpha = \pm\frac{1}{2}]_p$, will only be seen in Ho and Tm (cf. sect. 5), provided that their deformation is comparable to that of the odd-odd nuclei. Furthermore, the detectable signature splitting must be very small, because the inversion frequency lies not much higher than the backbending frequency. In the $[i_{13/2}]_n$ $[h_{11/2}]_p$ bands of the odd-odd nuclei both the first neutron (at ω_1(n)) and first proton (at $\omega_1(p)$) backbending are blocked. The first bandcrossing to be expected is therefore that at ω_2(n), which is due to the alignment of a neutron pair. The inversion frequency does not exceed this backbinding frequency except in ^{158}Tm. The frequency shown for this nucleus is obtained by extrapolating the curve in fig. 5. In fact the highest observed states in ^{158}Tm indicate the onset of a backbending [29]). (These points are not included in fig. 5, since they do not correspond to a pure configuration.)

The theoretically predicted band crossing frequencies are systematically too low. The band-crossing frequencies depend on the pairing gap and are therefore configuration dependent. With our assumption of a reduced pairing gap ($\Delta = 0.8\Delta_{o.e.}$), it is inevitable that we will get a too low value for the first

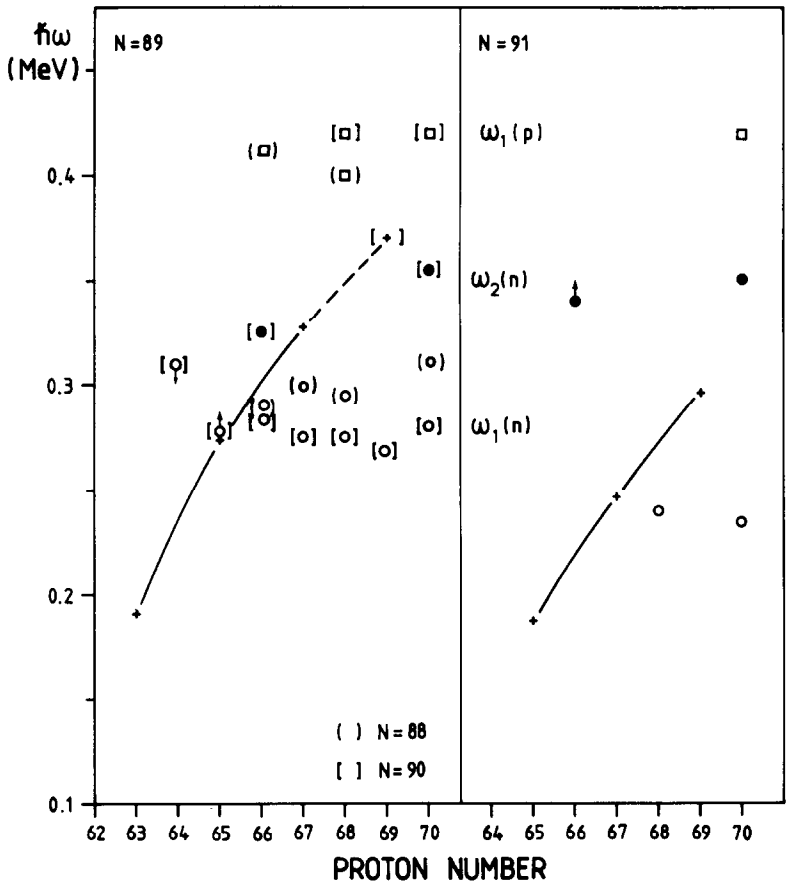

Fig. 11. Summary of experimentally known signature inversion frequencies (+) and band-crossing frequencies for some $N = 88$, 89, 90, 91 isotones. When a particular band crossing has been observed in more than one configuration in a nucleus an average value is shown. The data for the band-crossing frequencies are taken from the open litterature, except for ^{158}Yb [ref. [32])].

backbending frequencies (ω_1(n) and ω_1(p)), but the second neutron backbending frequency should be reasonably well reproduced. This is at least the case for the well-deformed rare-earth nuclei. We see, however, by comparing figs. 3c and 11 that the ω_2(n) crossing is calculated about 25 keV too low. A similar discrepancy occurs in the proton system, where the second proton crossing is calculated to fall below the frequency observed in experiment for the first proton crossing (ω_1(p)). We could improve the agreement by choosing a considerably larger Δ-value, but this would destroy the good agreement in alignment for the $N = 89$ isotones (cf. fig. 4). We believe that these problems are related to the problems found in describing the g-s crossing in ^{160}Yb in ref. [26]) where both the pairing field and the deformation were treated self-consistently. It is however impossible to judge

whether these problems, if properly understood, can lead to any modifications of the results obtained in this paper.

9. Summary

We have demonstrated that the signature splitting of the lowest quasiparticle levels of a high-j shell is inverted in a limited frequency interval for certain positions of the Fermi surface, provided that the deformation is triaxial and lies in the sectors $0 < \gamma < 60°$ or $-120° < \gamma < -60°$. We have discussed in what regions of the nuclear chart such deformations can be expected in combination with the proper position of the Fermi surface, and found that all the experimentally observed examples of signature inversion lie in precisely those regions.

By fitting the theoretical routhians to the experimentally observed signature splitting in odd-odd nuclei in the $N \approx 90$ mass region we found γ-values in the range $5° < \gamma < 25°$. Calculations performed at the deformations determined in this way reproduce quite well the experimentally observed spectra. We therefore believe that the estimated deformations are reasonable, although effects other than triaxiality might be of importance for the inverted signature splitting.

The signature inversion is a very striking phenomenon, which is immediately revealed in the experimental data, in particular if the observed region includes the inversion frequency. It is therefore a very useful indicator for the appearance of triaxial shapes in rotating γ-soft nuclei.

This work was partly sponsored by the Division of Basic Energy Sciences, US Department of Energy, under the contract W-7405-eng-26 with the Union Carbide Corporation.

References

1) A. Bohr and B. R. Mottelson, Proc. Int. Conf. on nuclear structure, Tokyo, Sept. 1977, J. Phys. Soc. Japan Suppl. **44** (1978) 157
2) F. S. Stephens, Rev. Mod. Phys. **47** (1975) 43
3) J. Meyer-ter-Vehn, Nucl. Phys. **A249** (1975) 111, 141
4) R. Bengtsson, F. R. May and J. A. Pinston, Proc. XX Int. Winter Meeting on nuclear physics, Bormio, Italy, Jan. 1982, p. 144
5) S. E. Larsson, G. Leander and I. Ragnarsson, Nucl. Phys. **A307** (1978) 189
6) J. A. Pinston, R. Bengtsson, E. Monnand, F. Schussler and D. Barneoud, Nucl. Phys. **A361** (1981) 464
7) R. Bengtsson, J. A. Pinston, D. Barneoud, E. Monnand and F. Schussler, Nucl. Phys. **A389** (1982) 158
8) J. D. Garrett, Proc. XX Int. Winter Meeting on nuclear physics, Bormio, Italy, Jan. 1982, p. 1
9) I. Hamamoto and B. R. Mottelson, Phys. Lett. **127B** (1983) 281
10) S. Frauendorf and F. R. May, Phys. Lett. **125B** (1983) 245
11) I. Ragnarsson, A. Sobiczewski, R. K. Sheline, S. E. Larsson and B. Nerlo-Pomorska, Nucl. Phys. **A233** (1974) 329

12) R. Bengtsson, P. Möller, J. R. Nix and J.-Y. Zhang, Phys. Scripta to be published
13) G. A. Leander, S. Frauendorf and F. R. May, Proc. Int. Conf. on high angular momentum properties of nuclei, Oak Ridge, USA, Nov. 1982, ed. N. R. Johnson (Harwood, New York, 1983) p. 281
14) A. André *et al.*, private communication, and to be published
15) J. A. Pinston *et al.*, private communication, and to be published
16) A. Neskakis, R. M. Lieder, H. Beuscher, Y. Gono, D. R. Haenni and M. Mueller-Veggian, Nucl. Phys. **A390** (1982) 53;
A. Neskakis, H. Beuscher, B. Bochev, T. Kutsarova, R. M. Lieder, T. Morek and F. R. May, Abstract for the Int. Conf. on nuclear physics, Florence, Italy (1983)
17) W. Neumann, L. Cleemann, J. Eberth, T. Heck, G. S. Li, M. Nolte and J. Roth, Abstracts to the Conf. on high angular momentum properties of nuclei, Oak Ridge, USA, Nov. 1982, p. 66
18) J. Doering, G. Winter, L. Funke, P. Kemnitz and E. Will, Z. Phys. **A305** (1982) 365
19) G. B. Hagemann, J. D. Garrett, B. Herskind, G. Sletten, P. O. Tjøm, A. Henriquez, F. Ingebretsen, J. Rekstad, G. Løvhøiden and F. Thorsteinsen, Phys. Rev. **C25** (1982) 3224;
J. D. Garrett, G. Hagemann, B. Herskind, J. Kownacki and P. O. Tjøm, Proc. Nordic Meeting on nuclear physics (Fuglsø, Denmark, 1982), Phys. Scripta, to be published
20) R. Holzmann, J. Kuzminski, M. Loiselet, M. A. Van Hove and J. Vervier, Phys. Rev. Lett. **50** (1983) 1834;
L. L. Riedinger, L. H. Courtney, A. J. Larabee, J. C. Waddington, M. P. Fewell, N. R. Johnson, I. Y. Lee and F. K. McGowan, Abstracts to the Conf. on high angular momentum properties of nuclei, Oak Ridge, USA, Nov. 1982, p. 4
21 C. A. Fields, K. H. Hicks, R. A. Ristinen, F. W. N. de Boer, L. K. Peker and P. M. Walker, Phys. Rev. **C26** (1982) 290
22) R. Bengtsson and S. Frauendorf, Nucl. Phys. **A327** (1979) 139
23) A. H. Wapstra and K. Bos, Atom. Nucl. Data Tables **19** (1977) 175
24) J. P. Boisson, R. Piepenbring and W. Ogle, Phys. Reports **C26** (1976) 99
25) R. Bengtsson and H. Frisk, to be published
26) R. Bengtsson, Y.-S. Chen, J.-Y. Zhang and S. Åberg, Nucl. Phys. **A405** (1983) 221
27) S. G. Nilsson, C. F. Tsang, A. Sobiczewski, Z. Szymański, S. Wycech, C. Gustafsson, I.-L. Lamm, P. Möller and B. Nilsson, Nucl. Phys. **A131** (1969) 1
28) R. Bengtsson and J.-Y. Zhang, Proc. Nucl. Phys. Workshop, Trieste, Italy, Oct. 1981, ed. C. H. Dasso, p. 165, and to be published
29) S. Drissi, S. André, J. Genevey, V. Barci, A. Gizon, J. Gizon, J. A. Pinston, J. Jastrzebski, R. Kossakowski and Z. Preibisz, Z. Phys. **A302** (1981) 361;
A. André *et al.* private communication, and to be published
30) G. Løvhøiden Phys. Scripta **25** (1982) 459
31) N. Rizk and J. Boutlet, J. de Phys. Lett. **37** (1976) 197
32) C. Baktash, private communication (Sept. 1983)